Broadband High Gain SIW Cavity-Backed Circular Polarized Array Antenna

Dong-Fang Guan, Can Ding, Zu-Ping Qian, Ying-Song Zhang, Y. Jay Guo, and Ke Gong

***Abstract*—A circularly-polarized (CP) 4×4 array antenna based on substrate integrated waveguide (SIW) technology is presented. Circular polarization is achieved by applying the sequential rotation technique (SRT) with a well designed sequential feed network and linear-polarized array elements. The proposed 4×4 array has a wide axial ratio (AR) bandwidth of 14% from 18.3 GHz to 21.1 GHz with gain >13 dBic. Then the array is expanded to achieve higher gains. A 16×16-element array is designed, fabricated, and tested. Test results show that the 16×16 array has an AR bandwidth of 13.8% from 18.5 GHz to 21.25 GHz and a peak gain of 25.9 dBic at 20.5 GHz.**

***Index Terms*—Antenna array, circular polarization, high gain, substrate integrated waveguide (SIW).**

I. Introduction

Owing to its resistance to polarization mismatch and multi-path effects, circularly polarized (CP) antennas are widely used in wireless communications. Generally speaking, there are two methods to achieve circular polarization for planar array antennas. One is to employ CP antenna elements in an array and the other is to use linearly-polarized (LP) antenna elements with specially designed feed network. In fact, the axial ratio (AR) bandwidth of an array mainly depends on the feed network. To achieve wideband circular polarization, sequential rotation technique (SRT) is a favored choice, where antenna elements are fed by uniform magnitude and progressive phase shifts of 90^o [1-2].

Microstrip technologies have been extensively utilized in SRT due to the advantages of compact structure and design flexibility of microstrip lines [3]-[6]. However, the gain of microstrip arrays is limited by losses in microstrip line feed networks, and the losses can be significant when the arrays are very large. Metallic waveguides with minor losses can achieve high efficiencies [7]-[8], but the design complexity makes them difficult to employ SRT. Recently, the substrate integrated waveguide (SIW) technology has been employed to design CP arrays [9]-[12]. Compared to the microstrip and metallic waveguide structures, SIW technology provides more flexibility in employing SRT, which is attributed to its advantages of compact structure, low loss, and easiness in controlling the output phases [11]-[12]. Moreover, SIW helps to suppress mutual coupling between array elements due to the closed walls in SIW cavities [10]. In [11], SIW power dividers with additional phase-delay lines were employed to build a sequential feed network to improve AR bandwidth. A 4×4-element SIW CP cavity-backed array was proposed in [12], which achieved a wide AR bandwidth by employing a double-layer SIW sequential network. However, the gains achieved by these SIW CP arrays are limited. To the authors' knowledge, the highest gain realized by the SIW CP planar arrays is 17.9 dBic. High gain could be achieved by expanding the array, but the major challenge is to maintain wide AR bandwidth and compact structure when the array expands.

A broadband 4×4 CP array antenna employing a novel compact SIW feed network with SRT is proposed in this communication. Then the 4×4 array is expanded to a 16×16 array to achieve higher gain. Owing to the proposed novel SRT feed network based on SIW, the bandwidth and compactness remain at the same level in the larger scale array. The rest of communication is organized as follows. The SIW based compact and wideband 4×4 CP array is presented in Section II. In section III, a 16×16 CP array is designed based on the proposed 4×4 CP array and the measurements of a fabricated array are presented. Section V draws the conclusion.

This work was supported in part by the National Science Foundation of China under Grant 61271103 and in part by the Open Project of State Key Laboratory of Millimeter Waves, Southeast University China under Grant K201515.

D. F. Guan, Z. P. Qian, and Y. S. Zhang are with the College of Communications Engineering, PLA University of Science and Technology, Nanjing 210007, China (e-mail:gdfguandongfang@163.com).

C. Ding and Y. Jay Guo are with the Global Big Data Technologies Centre, University of Technology Sydney (UTS), Australia.

K. Gong is with the College of Physics and Electronic Engineering, Xinyang Normal University, Xinyang 464000, China.

D. F. Guan, Y. S. Zhang, and K. Gong are also with the State Key Laboratory of Millimeter Waves, Southeast University, Nanjing 210096, China.

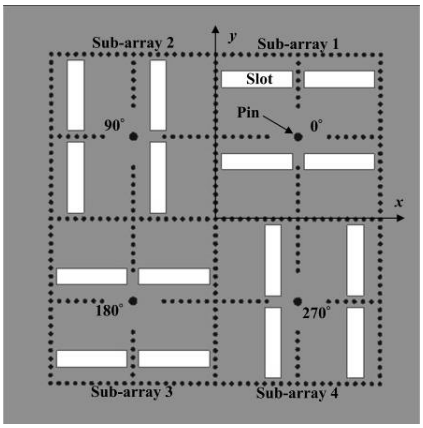

Fig. 1 Geometry of the array elements.

II. 4×4 Array Design

The 4×4 SIW CP array consisting of two layers are designed on Rogers-Duroid 5880 with thickness of 1.5 mm and 0.5 mm, respectively, as shown in Figs. 1 and 2. The top layer employs four LP SIW 2×2 sub-arrays as radiating elements, and the bottom layer is a compact sequential feed network.

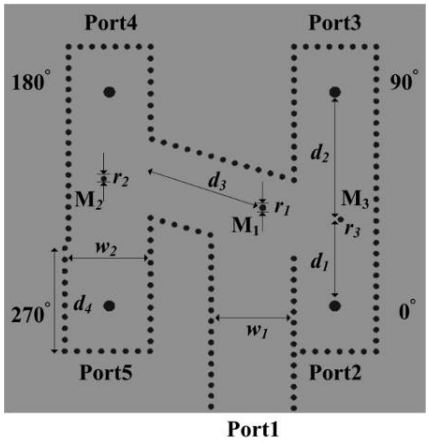

Fig. 2 Geometry of the sequential feed network. The parameters of the feed network are fixed as d_1=8.1 mm, d_2=11.9 mm, d_3=10.6 mm, d_4=9.6 mm, w_1 =6.8 mm,w_2=7.1 mm, r_1=0.3 mm,r_2= r_3=0.25 mm.

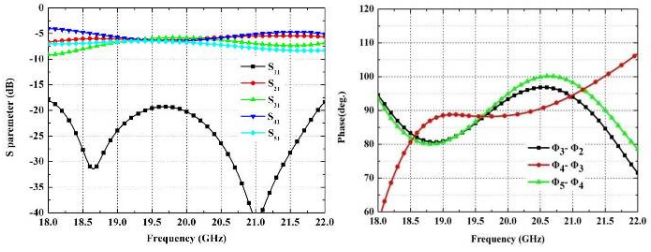

(a) (b)

Fig. 3 Amplitude and phase characteristics of the sequential feed network.

In Fig. 1, four 2×2 sub-arrays are placed with sequential rotation in correspondence with the bottom layer feed network. Each 2×2 sub-array is composed of four SIW cavities, which are coupled by inductive windows, and fed by a Pin located at the centre. There is a rectangular slot etched on the top of each cavity, so that the energy can radiate out. The 2×2 sub-array was studied in our previous work [13]. In this communication, it is chosen due to its broad bandwidth and compact structure.

The proposed SIW-based sequential feed network is shown in Fig. 2. It can be regarded as an unsymmetrical H-type four-way power divider. Port 1 is the input port and Ports 2 to 5 are the output ports with Pins to feed antenna sub-arrays in the upper layer. Metallic posts labeled as M_1, M_2 and M_3 are inserted in the power dividers for impedance matching. For the sake of clarity, here we define the current phase at Port n as Φ_n, for n = 2, 3, 4, 5. The design goal is to have progressive phase shifts between the output ports (Φ_{n+1}- Φ_n= 90°, for n = 2, 3, 4). The phase sequential rotation is realized by adjusting relevant dimensions. Detailed design processes are presented as follows.

A 90° phase shift between Ports 2 and 3 can be achieved by setting d_2-d_1=λ/4, where λ is the wavelength in the SIW line at the centre frequency, and a 90° phase shift between Ports 4 and 5 is obtained in the same manner. Then, the input SIW line is moved away from the middle to the right, thus resulting in a phase shift between the left and right branches. A 180° phase delay can be obtained by tuning d_3. It is noted that the position change of the input SIW line also affects the phase shift between Ports 4 and 5. Therefore, slight modification to

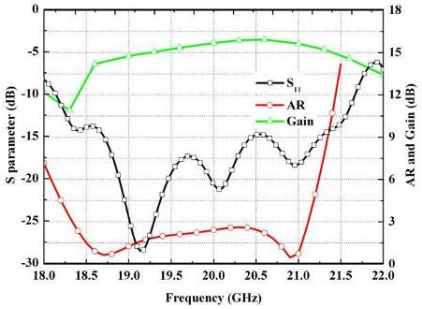

Fig. 4 Simulated reflection coefficient, AR, and gain of the 4×4 array.

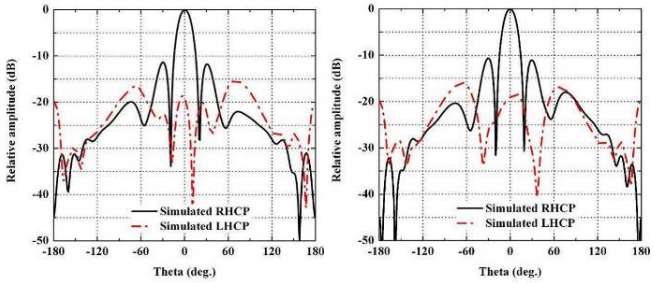

(a) (b)

Fig. 5 Simulated radiation patterns of the 4×4 array at 20 GHz, (a) *xz*-plane, (b) *yz*-plane.

the left branch is required to compensate for the phase error. This is realized by introducing a built-in phase shifter with an optimized width of w_2 and length of d_4. Finally, optimization on the radius of the metallic posts (r_1, r_2 and r_3) is made to achieve good impedance matching.

The dimensions of the sequential feed network are presented in the caption of Fig. 2, which are the optimized results obtained in HFSS considering all the constraints. The simulated amplitude and phase characteristics of the sequential feed network are shown in Fig. 3. The transmission coefficients S_{n1} (n = 2, 3, 4, 5) are approximately -6 dB at the centre frequency 20 GHz and the amplitude imbalance is within ±2 dB from 18.5 to 21.5 GHz. The reflection coefficient is < -15 dB over the operating band. Fig. 3(b) shows the simulated phase differences between the output ports. As shown in this figure, progressive phase shifts of 90° are obtained between the Ports 2 to 5 at the centre frequency 20 GHz and the phase error is within ±10° from 18.5 GHz to 21.5 GHz. The results indicate that this feed network is able to provide the required sequential phase rotation across the band from 18.5 GHz to 21.5 GHz (15%).

The simulated reflection coefficient S_{11}, AR, and gain of the proposed array are presented in Fig. 4. The 3-dB AR bandwidth of the array is 14% from 18.3 GHz to 21.1 GHz. In this band, the S_{11} is < -14 dB and the realized gain is > 13 dBic with a peak gain of 15.9 dBic at 20.6 GHz. Fig. 5 shows the simulated normalized radiation patterns in *xz*- and *yz*-planes at 20 GHz. As observed from Fig. 5, the 3-dB beamwidths in both *xz*-and *yz*-planes are about 18°, the side lobe levels (SLL) and the cross-polarization levels are < -11 dB and < -18 dB, respectively. The simulated results show that the CP array has a wide AR bandwidth with superior radiation performance.

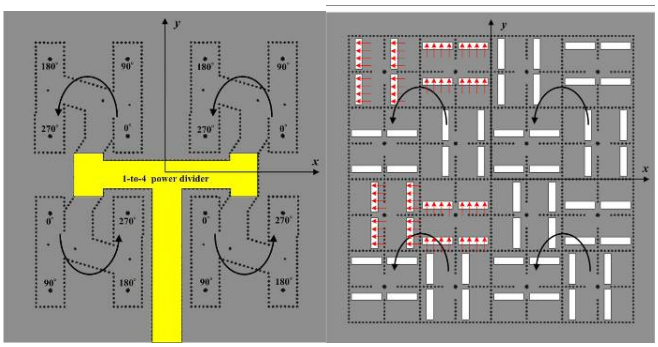

(a) (b)

Fig. 6 Geometry of the 8×8 array, (a) bottom layer, (b) top layer.

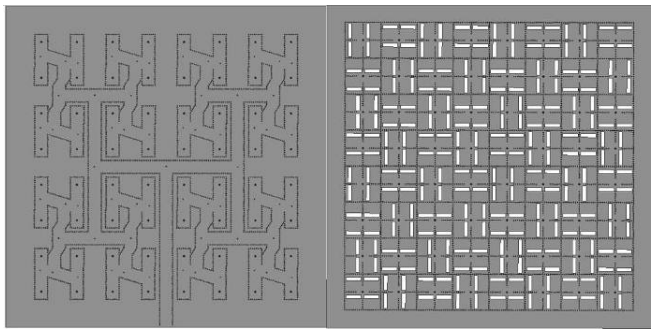

(a) (b)

Fig. 7 Geometry of the 16×16 array, (a) bottom layer, (b) top layer.

III. 16×16 Array Design

The 4×4 array described in Section II is easily expandable as the feed network is completely underneath the radiators. Fig. 6(a) and 6(b) show the feed network and the radiating layer of an 8×8 array expanded from the 4×4 array. Four sequential feed networks are combined by a 1-to-4 H-type power divider and arranged in the way shown in Fig. 6(a). The sequential power divider shown in Fig. 2 is hereafter referred to as sub-power divider for the sake of brevity. To make the whole feed network compact and scalable, two sub-power dividers at the bottom are rotated by 180^o with respect to those at the top. However, it is noted that the sub-power divider shown in Fig. 2 is not rotationally symmetric. Phase differences of 180^o (phase reversal) are observed between the outputs of the sub-feeds at the top and bottom half of the whole feed network. This leads to a null at the boreside direction if identical radiators are connected to the feed network.

To overcome the problem, the phase reversal should be removed. We can change the orientations of the antenna elements on the top layer to compensate for the phase reversal introduced by the bottom feed network. As can be seen in Fig. 6(b), the sub-arrays at the bottom half of the array are rotated by 180^o with respect to the corresponding ones at the top half array to create the phase reversal. This way, the phase reversals from the feed layer and radiation layer are cancelled out with each other.

It is noted that the 8×8 array shown in Fig. 6 are rotationally symmetric. Therefore, larger arrays could be obtained by simply duplicating the 8×8 array in two dimensions and connecting them with H-type SIW power dividers. Fig. 7(a) and 7(b) illustrate the geometries of the top and bottom layers of a 16×16 array. It was also fabricated and tested. Fig. 8 shows the 16×16 array prototype. It has an array size of 180×190 mm^2. To measure the array, a 50-Ω microstrip line with a tapered transition was added to the end of the input port to provide impedance matching. The simulated and measured reflection coefficients of the array antenna are shown in Fig. 9. The measured impedance bandwidth is 15.9% from 18.5 GHz to 21.7 GHz, which is slightly narrower than the simulated one. There exist some ripples in the measured S_{11}, which are mainly attributed to the reflections between the feed network and the top layer.

Fig. 8 The 16×16 array prototype.

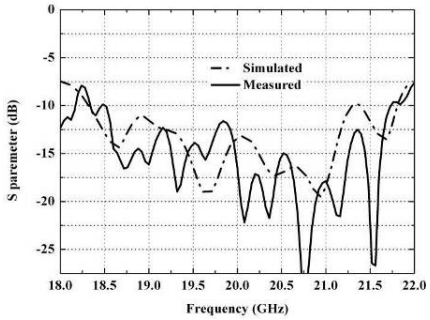

Fig. 9 Simulated and measured reflection coefficients of the 16×16 array.

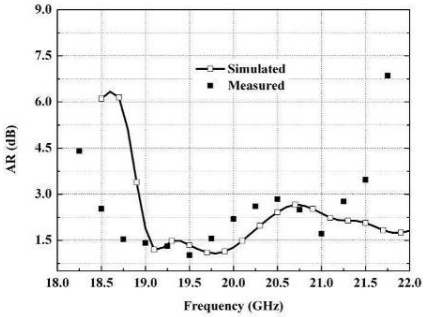

Fig. 10 Simulated and measured AR of the 16×16 array.

The AR, gain and radiation patterns of the array were measured in a chamber with far-field setup from 18.25 GHz to 21.75 GHz. The measured AR and gain are compared with the simulated ones in Figs. 10 and 11, respectively. As shown in Fig. 10, the measured 3-dB AR bandwidth is 13.8% from 18.5 GHz to 21.25 GHz. The measured AR bandwidth is lower than the simulated one, which is attributed to the fabrication tolerance and measurement errors. According to Fig. 11, the

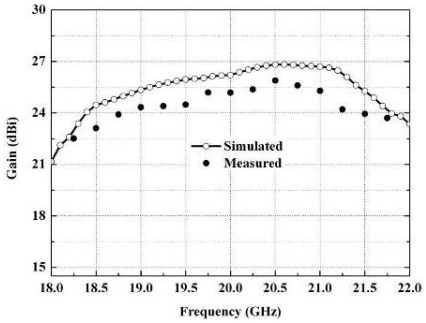

Fig. 11 Simulated and measured gains of the 16×16 array.

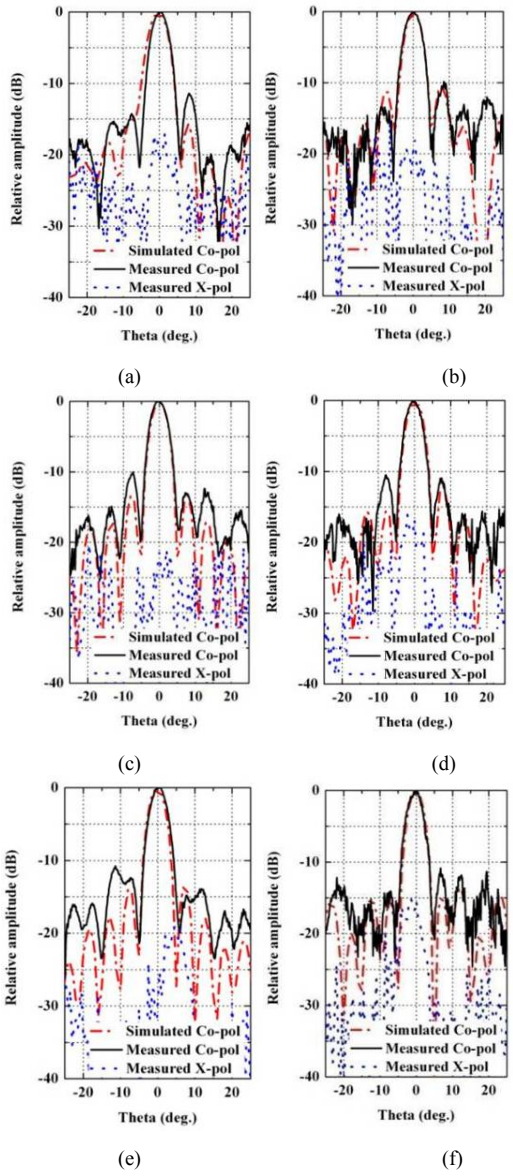

Fig. 12 Simulated and measured normalized radiation patterns of the 16×16 array, (a) *xz*-plane at 19 GHz, (b) *yz*-plane at 19 GHz, (c) *xz*-plane at 20 GHz, (d) *yz*-plane at 20 GHz, (e) *xz*-plane at 21 GHz, (f) *yz*-plane at 21 GHz.

measured gain agrees well with the simulated one with a discrepancy of 1 dB. The measured gain is from 22.5 dBic to 25.9 dBic and the peak gain is 25.9 dBic at 20.5 GHz.

Fig. 12 shows the simulated and measured radiation patterns in *xz*- and *yz*-planes at 19, 20, and 21 GHz, respectively. As shown in Fig. 12, the measured right-hand circular polarization (RHCP) patterns are in good agreement with the simulate ones. The 3-dB beamwidths in both *xz*- and *yz*-planes are approximately 5° and the measured SLLs are < -10 dB across the entire operating band. The measured cross-polarization levels are < -10 dB for all the frequencies.

IV. Conclusion

In this communication, a large-scale SIW-based CP array is proposed. The CP array uses linear polarized 2×2 SIW sub-arrays as radiating elements and employs a novel sequential rotation SIW feed network. The obtained 4×4 array has a wide AR bandwidth and satisfactory radiation performance. Then it is expanded to a 16×16 array. The measured results of the 16×16 array show that a higher gain is achieved while the impedance bandwidth and AR bandwidth are maintained.

References

[1] R.C. Hansen, "Phased array antennas", Wiley, 1998.

[2] J. Huang, "A technique for an array to generate circular polarization with linearly polarized elements", IEEE Trans. Antennas and Propag.,vol. 34, no. 9, pp. 1113-1124, Sep. 1986.

[3] J. Huang, "Ka-band circularly polarized high-gain microstrip array antenna," IEEE Trans. Antennas and Propag., vol. 43, no. 1, 1995, pp. 113–116.

[4] P.S. Hall and C.M. Hall, "Coplanar corporate feed effects in microstrip patch array design", IEE Proc., vol. 135H, 1988, pp.180-186.

[5] P.S. Hall & M.S. Smith, "Sequentially rotated arrays with reduced sidelobe levels', Proc. IEEMAP, vol. 141, 1994, pp. 321-325.

[6] P. Brachat& J.M. Baracco, "Dual-polarization slot-coupled printed antennas fed by stripline", IEEE Trans. Antennas and Propagation, vol. 43, 1995, pp.738-742.

[7] D. Kim, J. Hirokawa, M. Ando, J. Takeuchi and A. Hirata, "64×64-element and 32×32-element slot array antennas using double-layer hollow-waveguide corporate-feed in the 120 GHz band," *IEEE Trans. Antennas Propag.*, vol. 62, no. 3, pp. 1507–1512, Mar. 2014.

[8] M. Zhang, J. Hirokawa, and M. Ando, "An E-band partially corporate feed uniform slot array with laminated quasi double-layer waveguide and virtual PMC terminations," *IEEE Trans. Antennas Propag.*, vol. 59, no. 5, pp. 1521-1527, May 2011.

[9] P. Chen, W. Hong, Z. Q. Kuai and J. F. Xu, "A substrate integrated waveguide circular polarized slot radiator and its linear array," *IEEE Antennas Wirel. Propag. Lett.*, vol. 8, pp. 120-123, 2009.

[10] A. B. Guntupalli and K. Wu, "60-GHz circularly polarized antenna array made in low-cost fabrication process," *IEEE Antennas Wirel. Propag. Lett.*, vol. 13, pp. 864-867, 2014.

[11] Eun-Young Jung, Jae W. Lee, Taek K. Lee, and Woo-Kyung Lee, "SIW-based array antennas with sequential feeding for X-band satellite communication," *IEEE Trans. Antennas Propag.*, vol. 60, no. 8, pp. 3632-3638, August 2012.

[12] Y. Lang, S. W. Qu, and J. X. Chen, "Wideband circularly polarized substrate integrated cavity-backed antenna array," *IEEE Antennas Wirel. Propag. Lett.*, vol. 13, pp. 1513-1516, 2014.

[13] D. F. Guan, C. Ding, Z. P. Qian, Y. S. Zhang, W. Q. Cao, and Eryk Dutkiewicz, "A SIW Based Large-Scale Corporate-Feed Array Antenna," *IEEE Trans. Antennas Propag.*, vol. 63, no. 7, pp. 2969–2976, Jul. 2015.